Temporal Monitoring and Predicting of the Abundance of Malaria Vectors Using Time Series Analysis of Remote Sensing Data through Google Earth Engine

Fahimeh Youssefi (fahimeh.y@gmail.com)
K N Toosi University of Technology Faculty of Geodesy and Geomatics Engineering
https://orcid.org/0000-0002-7265-3866
Mohmmad Javad Valadan Zoej
K N Toosi University of Technology Faculty of Geodesy and Geomatics Engineering
Ahmad Ali Hanafi-Bojd
Tehran University of Medical Sciences
Alireza Borhani Darian
K N Toosi University of Technology Faculty of Civil Engineering
Mehdi Khaki
University of Newcastle
Alireza Safdari Nezhad
Tafresh University

Research

Keywords: Malaria, Remote sensing, Climate, Anopheles, Google Earth Engine, Hydroclimate time series

Posted Date: December 3rd, 2021

DOI: https://doi.org/10.21203/rs.3.rs-1103260/v1

Temporal monitoring and predicting of the abundance of malaria vectors using time series analysis of remote sensing data through Google Earth Engine

Fahimeh Youssefi[1]*, Mohmmad Javad Valadan Zoej[†1], Ahmad Ali Hanafi-Bojd[†2,3], Alireza Borhani Darian[††4], Mehdi Khaki[††5], Alireza Safdari Nezhad[6]

† Mohmmad Javad Valadan Zoej and Ahmad Ali Hanafi-Bojd contributed equally to this work.

†† Alireza Borhani Darian and Mehdi Khaki contributed equally to this work.

[1] Department of Photogrammetry and Remote Sensing, K.N.Toosi University of Technology, Tehran, Iran

[2] Zoonoses Research Center, Tehran University of Medical Science, Tehran, Iran

[3] Department of Medical Entomology & Vector Control, School of Public Health, Tehran University of Medical Sciences, Tehran, Iran

[4] Department of Water Resource, K.N.Toosi University of Technology, Tehran, Iran

[5] School of Engineering, University of Newcastle, Callaghan, Australia

[6] Department of Geomatics, Tafresh University, Arak, Iran

*Correspondence: youssefi@email.kntu.ac.ir

MJVZ: valadanzouj@kntu.ac.ir

AAHB: aahanafibojd@tums.ac.ir

ABD: borhani@kntu.ac.ir

MK: Mehdi.Khaki@newcastle.edu.au

ASN: safdarinezhad@tafreshu.ac.ir

Abstract

Background: In many studies in the field of malaria, environmental factors have been acquired in single-time, multi-time or a short time series using remote sensing and meteorological data. Selecting the best periods of the year to monitor the habitats of *Anopheles* larvae can be effective in better and faster control of malaria outbreak.

Methods: In this article, high-risk times for three regions in Iran, including Qaleh-Ganj, Sarbaz and Bashagard counties with history of malaria prevalence had been estimated. For this purpose, a series of environmental factors affecting the growth and survival of *Anopheles* had been used over a seven-year period through the GEE. Environmental factors used in this study include NDVI and LST extracted from Landsat-8 satellite images, daily precipitation data from PERSIANN-CDR, soil moisture data from NASA-USDA Enhanced SMAP, ET data from MODIS sensor, and vegetation health indices included TCI and VCI extracted from MODIS sensors. All these parameters were extracted on a monthly average for seven years and, their results were fused at the decision level using majority voting method to estimate high-risk time in a year.

Results: The results of this study indicated that there were two high-risk times for all three study areas in a year to increase the abundance of *Anopheles* mosquitoes. The first peak occurred from late winter to late spring and the second peak from late summer to mid-autumn. If there is a malaria patient in the area, after the end of the *Anopheles* larvae growth period, the disease will spread throughout the region. Further evaluation of the results against the entomological data available in previous studies showed that the high-risk times predicted in this study were consistent with the increase in the abundance of *Anopheles* mosquitoes in the study areas.

Conclusions: The proposed method is very useful for temporal prediction of the increase of the abundance of *Anopheles* mosquitoes and also the use of optimal data with the aim of monitoring the exact location of *Anopheles* habitats. This study extracted high-risk time based on the analysis of the time series of remote sensing data.

Keywords: Malaria; Remote sensing; Climate; *Anopheles*; Google Earth Engine; Hydroclimate time series

Background

Malaria is an infectious disease transmitted by the *Anopheles* mosquito and claims millions of lives globally every year [1]. The pattern of malaria transmission varies markedly from region to region, depending on climate and biogeography [2]. Although malaria has been successfully eradicated in many parts of the world in recent decades, *Anopheles* mosquitoes have not become extinct. Besides, there is still the risk of malaria transmission in areas where *Anopheles* mosquitoes live [3]. A recent study has shown that targeting the *Anopheles* larvae can be an effective tool in the fight against malaria [4]. The growth of *Anopheles* mosquitoes from eggs to larvae and finally to adult mosquitoes occurs in water bodies at a suitable temperature, so the

abundance of *Anopheles* mosquito are closely associated with the availability of precipitation, temperature and humidity [4-8].

Fortunately, malaria cases in Iran have dropped to zero in the last three years [9]. Therefore, according to the malaria elimination guidelines, the country is a candidate of receiving the malaria elimination certificate. As the incidence of the disease decreases, it is expected that the budget allocated to the field-based operations, such as monitoring the activity of larvae and adults of malaria vectors, which has previously been performed regularly in endemic areas of the disease, will be reduced. Therefore, access to the up-to-date data on *Anopheles* abundance and the accurate time of their temporal activity should be done through alternative means that are less expensive but more accurate. One of these ways is to study the environmental factors affecting the activity of malaria vector mosquitoes. Due to the fact that some environmental and climatic parameters affect the abundance of *Anopheles* mosquitoes, analysis and monitoring of climatic trends in the region will be effective in determining the accurate time for vector control interventions. The climatic trend of each region will be obtained by long-term monitoring of its climate data. Some studies on effective environmental parameters have shown that precipitation has the greatest impact on the prevalence of malaria [10-11]. This phenomenon occurs due to the storage of water in the pits and water bodies after rainfall. Precipitations is necessary to produce breeding sites for the mosquito to complete its life cycle [12-13]. Moreover, temperature plays a vital role in the spreading of vector borne diseases. Temperature between 13-35^{o}C is suitable for *Anopheles* mosquito breeding [14-17]. Land Surface Temperature (LST) is one of the key parameters that can provide valuable information about the thermal characteristics of the ground, atmospheric effects of spectral radiation and bulk emissivity of the mixture of materials within the scene. Various satellites such as NOAA,

Landsat, Terra, etc. have been designed for temperature studies. LST is positively associated with malaria incidence [12, 18]. In addition to precipitation, moisture and LST, vegetation indices are also considered as one of the important environmental factors associated with the prevalence of malaria [3, 11, 19-20]. Temporal variation in Normalized Difference Vegetation Index (NDVI) reflects temporal agricultural and phenology changes and also tracks fluctuations in temperature and precipitation.

Vegetation indices, thus, provide an indirect measurement of the environmental pattern that affects the population of *Anopheles* mosquitoes. On the other hand, epidemiologic data of malaria cases are correlated with satellite based vegetation health (VH) indices [21-23]. The VH indices were represented by the Thermal Condition Index (TCI) and Vegetation Condition Index (VCI). The VCI and TCI estimate moisture and thermal conditions, respectively. Rahman et al. [21] found that the number of malaria cases was more sensitive to thermal (e.g., TCI) than moisture (e.g., VCI) conditions. Given that water areas are the main habitat for the growth of *Anopheles* larvae, the water index such as Normalized Difference Water Index (NDWI) can also be considered as an effective parameter in the seasonal study of malaria prevalence [6, 11, 24]. The index is also an indirect proxy for precipitation and humidity [25].

In previous researches reviewed, not all effective parameters were analyzed simultaneously over a period of several years. In addition, field observations can be more accurate for monitoring effective factors, but the accessibility to this data is very limited in the long run and over large areas. Certainly, in order to accurately predict the increase of the abundance of *Anopheles* mosquitoes, simultaneous examination of all parameters is important, and this analyzing should be done in a long period of time in the region [6, 26]. Because most of the parameters affecting the increase of the abundance of *Anopheles* mosquitoes are climatic

parameters, and long-term analysis provides more accurate information about the climatic behavior of the region. If only one year is examined, the possibility of errors in the high-risk time prediction will occur. Some years had experienced drought and the results of these years were slightly different from the typical climatic behavior of the region. Also, high-risk times in a year can be detected using time series remote sensing data analysis. Therefore, by extracting the climatic and trends of environmental factors, high-risk periods within a year can be predicted. In recent years, GEE has made it possible to analyze time series remote sensing data easily and in the shortest time by providing fast and accessible processing space and easy access to free remote sensing data [27-28]. The aim of this study was to predict the high-risk time of increasing number of *Anopheles* mosquitoes and seasonal outbreak of malaria using time series of remote sensing data in three study areas of Qaleh-Ganj, Sarbaz and Bashagard in Iran.

Methods

In this research, high-risk times in a year in three study areas of Qaleh-Ganj, Sarbaz and Bashagard in Iran had been studied by monitoring satellite-derived environmental factors in a period of seven years. In this study, time series of precipitation, LST, surface and subsurface soil moisture, NDVI and VH indices were analyzed simultaneously using GEE (Google Earth Engine). In addition, the correlation between effective factors such as precipitation and soil moisture was studied for optimal selection of parameters. GEE had the ability to analyze the effective parameters on the abundance of *Anopheles* mosquitoes in the long run by providing a strong processing space as well as easy access to time series remote sensing data. Finally, based on the environmental and meteorological trend, high-risk periods for each study area was extracted and evaluated against entomological data [29-31].

Study area

According to research conducted in Iran [31-35], in recent years, cases of malaria have been observed in the three counties of Qaleh-Ganj, Sarbaz and Bashagard. These three counties have the potential to provide *Anopheles* mosquito larval habitats due to their subtropical climate and environmental conditions. Qaleh-Ganj county located at 27°31'33.43" Northing and 57°52'41.9" Easting in the south of Kerman Province, Sarbaz county located at 26°37'58.28" Northing and 61°15'30.01" Easting in the south-east of Sistan and Baluchestan Province, and Bashagard county located at 26°27'29.08" Northing and 57°54'7.39" Easting in the east of Hormozgan Province (Fig. 1). These study areas have hot weather and monsoon rains in mid-summer. The study period in all three study area was from 2014 to 2021.

Data and method

In this article, by processing the time series of effective factors in GEE in a period of seven years, high-risk time periods during a year have been predicted based on the regions' climate and meteorological trends. The flowchart of the proposed method is shown in Fig. 2. Six effective environmental factors including precipitation, soil moisture, NDVI, ET, VH indices and LST had been obtained from remote sensing data from 2014 to 2021. Each of these data had its own temporal resolution, so to equalize the temporal resolutions; the monthly average of each data was obtained. This would also be used to check for high-risk months. Then, by fusing the results of all effective factors in a period of seven years based on the majority voting decision, the high-risk months were identified in three study areas of Qaleh-Ganj, Sarbaz and Bashagard counties. Finally, the results were evaluated by the abundance of *Anopheles* mosquitoes which were observed in the study areas.

Remote sensing data with medium and low spatial resolution had been used due to high temporal resolution, being free, extended areas as well as relatively long study period (Table 1). The data used include Landsat-8 OLI/TIRS satellite images to extract LST, vegetation and health vegetation indices, PERSIANN-CDR data to extract precipitation, MOD16A2 Evapotranspiration/Latent Heat Flux product to monitor ET and NASA-USD Enhanced SMAP data to monitor soil moisture (Figure 3). All these data had been obtained as a time series for all three study areas of Sarbaz, Qaleh-Ganj and Bashagard from 2014 to 2021. The GEE, which is a cloud-based geospatial processing platform for large-scale environmental monitoring and analysis, was used to process the remote sensing data. This platform is a browser-based interactive development environment and a JavaScript programming interface provides access to a wide range of satellite products. Computations in this environment are performed through parallel processing in Google Cloud [28].

LST

Anopheles mosquitoes have different species and each of them grows and survives in a certain temperature range. In general, most of the *Anopheles* larvae species developed into adults at temperatures ranging from 13 to 35 ° C [14-17, 36]. In this research, LST time series from Landsat 8 OLI/TIR images were used to monitor land surface temperature changes. In order to calculate the surface temperature, first, it was necessary to apply the pre-processing on the images including applying cloud and shadow masks and also atmospheric and radiometric corrections. The NDVI was used (Eq. 1) to determine the emission capacity of the land surface. The effects of the atmosphere at spectral signatures and vegetation indices have been highlighted by Duggin and Piwinski [37]. Errors occurred by atmospheric effects influence the quality of the

information extracted from remote measurements, such as vegetation indices [38]. Therefore, surface reflectance images are used at this stage.

$$NDVI = \frac{NIR - Red}{NIR + Red} \quad \text{Eq. 1}$$

Where NIR and Red are equal to the near infrared and the red bands, respectively. After calculating the NDVI index, based on the obtained values, Land Surface Emissivity (LSE) was determined according to Table 2 [39].

The Brightness temperature (BT) is the temperature corresponding to the radiance received from the surface of a phenomenon or object by the sensor, which is obtained by the inverse of the Planck relation (Eq. 2).

$$BT = \frac{k_2}{\ln\frac{k_1}{L_\lambda} + 1} \quad \text{Eq. 2}$$

Where L_λ is equal to the spectral radiation, λ is the central wavelength of each band, and k_1 and k_2 are equal to the calibration coefficients of the sensor brightness temperature.

Then the surface temperature is calculated through Eq. 3 [39].

$$LST = \frac{BT}{1 + \left(\lambda \frac{BT}{\rho}\right)\ln(\varepsilon)} \quad \text{Eq. 3}$$

Where BT is the brightness temperature at the sensor, λ is the band wavelength, and ε is equal to the LSE (Table 1). ρ can also be calculated from Eq. 4.

$$\rho = \frac{hc}{s} = 1.438 \times 10^{-2}\, mk \quad \text{Eq. 4}$$

Where h is the Planck constant (6.626×10^{-34} Js), c is the speed of light (1.38×10^{-23}J/K) and s is the Boltzmann constant (2.998×10^{-8} m/s). Finally, in order to convert the LST unit from Kelvin to Celsius, the value of 273.15 is reduced.

Precipitation

One of the methods for estimating precipitation is the use of Precipitation Estimation from Remotely Sensed Information using PERSIANN-CDR data. PERSIANN-CDR provides daily rainfall estimates for the latitude band 60°S–60°N. PERSIANN-CDR is aimed at addressing the need for a consistent, long-term, high-resolution (0.25 degree), and global precipitation dataset for studying the changes and trends in daily precipitation, especially extreme precipitation events, due to climate change and natural variability [40]. In this study, in order to monitor the precipitation trend of the study areas, PERSIANN-CDR data from 2014 to 2021 were averaged on a monthly basis using GEE.

Soil Moisture

The National Aeronautics and Space Administration-United States Department of Agriculture (NASA-USDA) Enhanced Soil Moisture Active Passive (SMAP) global soil moisture data provides soil moisture information across the globe at 10-km spatial resolution. This dataset includes surface and subsurface soil moisture and was also created by integrating SMAP surface soil moisture satellite-derived observations into a modified two-layer Palmer model using a one-dimensional (1D) ensemble Kalman filter (EnKF) data assimilation approach. The integration of SMAP soil moisture observations helps to improve the model-based soil moisture prediction, especially in areas of the world that lack good quality precipitation data [41]. In order to study

changes in soil moisture over the period of seven years, the monthly average of surface and subsurface soil moisture were used in GEE over the study areas.

NDVI

One of the most widely used and the simplest vegetation indices, used to monitor vegetation changes, is the NDVI (Eq.1). As outlined in the literature, changes in this index are directly related to the prevalence of malaria. In this study, the NDVI had been extracted as a monthly average, from 2014 to 2021, using red and near infrared bands of the Landsat 8 OLI. This implementation had been done in the GEE for all study areas.

VH

The most widely used indicators of vegetation health and drought are VCI and TCI. If TCI increases and VCI decreases during the time, it means that drought has occurred in that area [42]. Apart from the fact that these two indicators are used in vegetation health and drought, they monitor vegetation and temperature in their equations in the long run; so they can also be used as an indicator of the ideal growth conditions of *Anopheles* mosquitoes. Decreasing the values of VCI over a long period of time indicates a decrease in vegetation moisture. This index compares the current NDVI to the range of values observed in a period of time. The VCI index is defined as follows (Eq. 5) [43-44].

$$VCI = \frac{NDVI_i - NDVI_{min}}{NDVI_{max} - NDVI_{min}} \quad \text{Eq. 5}$$

Where, $NDVI_{max}$ and $NDVI_{min}$ are equivalent to the maximum and minimum NDVI over the study period, respectively, and i represents the current year.

The TCI is used to monitor vegetation drought changes over a long period of time. This index is based on the relationship between actual (LST_i) and potential condition temperature (LST_{min}) and vegetation stress (LST_{max}) (Eq.6) [43-44].

$$TCI = \frac{LST_{max} - LST_i}{LST_{max} - LST_{min}} \quad \text{Eq.6}$$

Where, LST_{min} and LST_{max} are equivalent to the minimum and maximum LST over a period, respectively, and i represents the current year. The increasing trend of TCI in the long period of time demonstrates vegetation drought in the region [42]. In this research, the TCI and the VCI had been implemented as a time series from 2014 to 2021 for all study areas.

ET

The MOD16A2 Evapotranspiration/Latent Heat Flux product is an 8-day composite product produced at 500-meter pixel resolution by MODIS sensor. The algorithm used for the MOD16 data product collection is based on the logic of the Penman-Monteith equation, which includes inputs of daily meteorological reanalysis data along with MODIS remotely sensed data products such as vegetation property dynamics, albedo, and land cover [45]. The pixel values for the ET are the sum of all eight days within the composite period. Since the ET is related to soil moisture, water content of vegetation, temperature and precipitation, this component could also be one of the factors considered in the malaria prevalence. Therefore, in this study, the monthly average of ET changes from the MOD16A2 product in the seven-year period were applied using the GEE platform.

Data fusion

After calculating the monthly average of all seven parameters of NDVI, LST, ET, soil moisture, TCI, VCI and precipitation, their seven-year average per month was also determined. In this way, in a period of seven years, the climatic behavior of the region that affects the abundance of *Anopheles* mosquitoes was estimated. Then, in order to find high-risk months in which the necessary conditions were provided for the growth and development of *Anopheles* mosquitoes, fusing the results at the decision level was used. In this method, the majority voting condition was used in the final decision. Thus, if out of every seven parameters, four or more parameters occurred simultaneously in each month (in its peak interval), that month would be selected as the high-risk month. It should be noted that temperature has a definite role in this process and the appropriate temperature for *Anopheles* mosquitos' growth must be considered in the final decision.

Results

The time series of LST, precipitation, Soil moisture, NDVI, vegetation health indices and ET were implemented in GEE.

LST

LST is directly related to temperature; therefore, to investigate the time series of temperature, the monthly average LST from Landsat-8 OLI/TIR satellite images were extracted. The LST time series for the three study areas of Qaleh-Ganj, Sarbaz and Bashagard are shown in Fig. 4.

According to the comparison of LST in study areas, the average LST in different months of the year was approximately 10 °C higher than the average temperature reported from meteorological data in weather stations. Therefore, the suitable LST for the growth and survival of *Anopheles* mosquitoes approximately happened from 23 to 45 ° C.

The ideal temperature for the growth and survival of *Anopheles* mosquitoes for Qaleh-Ganj and Bashagard counties was from the beginning of February to the end of May and again from the beginning of September to the end of November. The suitable temperature range for Sarbaz County was slightly different, and the first peak continued until the end of June.

NDVI

Vegetation changes in study areas were analyzed using NDVI time series extracted from red and near infrared bands of Landsat-8 OLI images. In this process, surface reflectance images with cloud coverage of less than 5% were applied. As can be seen from Fig. 5, the NDVI values for all three study areas were very low and close to zero. These results indicate lack of vegetation in these areas.

In the county of Qaleh-Ganj, the NDVI peak occurred from February to May. In the counties of Sarbaz and Bashagard, the NDVI pattern was slightly different and two peaks were seen per year. In Bashagard, the first peak occurred from January to the end of June and, the second occurred from September to the end of December. This could be due to the cultivation of winter crops in the region. In Sarbaz, the first peak started from February to the end of May and the second peak started from September to the end of December.

Precipitation

Another important parameter in increasing the abundance of *Anopheles* was precipitation. The average daily precipitation chart in a month has been prepared using the daily precipitation data of PERSIANN-CDR in GEE from 2014 to 2021. The horizontal axis of the chart represented the months of a year and, its vertical axis was the average of precipitation in millimeters for each month.

As shown in Fig. 6(a), most precipitation in Qaleh-Ganj was between February to April, June to July and October to December. In Sarbaz, the amount of precipitation in the last seven years had been more than Qaleh-Ganj and Bashagard. In this county, the most rainfall occurred from January to May, July to August, and then the rainfall decreased until October. Also, moderate rainfall was observed from the middle of September to November (Fig. 6(b)). Bashagard had a similar precipitation chart to Qaleh-Ganj (Fig. 6(c)). Due to the close distance of these counties to each other, similar climatic conditions had occurred.

Soil moisture

Another effective environmental factor was soil moisture. Relative moisture affects the lifespan of *Anopheles* mosquitoes. Soil moisture of the study areas is shown in Fig. 7. In this figure, soil moisture was generated in two forms of Surface Soil Moisture (SSM) and SUbsurface Soil Moisture (SUSM) using the monthly averaging of NASA-USDA Enhanced SMAP time series data. Based on these results, the counties of Bashagard and Qaleh-Ganj had the highest levels of SSM and SUSM from February to the end of April and September to the end of December. It should be noted that the amounts of SSM and SUSM in Bashagard were more than the county of Qaleh-Ganj in the same months. In the county of Sarbaz, the SSM and SUSM were maximum from February to the end of April, but there was no heavy rain in November) Based on a survey of PERSIANN precipitation data) and the second peak was not observed. In addition, when there was a wet season in the region, the rain was heavier and more frequent in the year.

ET

The next factor is the total ET, which is related to the precipitation diagram (Figure 8). For all study areas, the amount of ET was high in January to May and October to December. In addition

to the mentioned months, ET was observed in July and August in Sarbaz. Due to the fact that the study areas had a warm and subtropical climate, soon after the precipitation increased, the rate of ET also increased.

VH

The last factor that was monitored in relation to the abundance of *Anopheles* mosquitoes was vegetation health indices. Monitoring the time series of these indices for a long time could also show the drought trend in the study areas. As shown in Fig. 9, fluctuations can be seen in these charts, which could be due to noisy data. Especially in the case of the TCI chart, the number of fluctuations is higher. Because of some reasons, such as the cloud, these data might be noisy. With the exception of Qaleh-Ganj, the other two counties did not show specific behavior in a year through the TCI. For Qaleh-Ganj, a peak was observed from February to September. In VCI charts, one peak occurred for both Qaleh-Ganj and Sarbaz. This peak was seen from February to November. There was no clear peak for Bashagard.

Data fusion

Finally, all the above results for the parameters of temperature, NDVI, precipitation, soil moisture, ET and VH indices are given in Fig. 10. Temperature plays an essential role in the growth of *Anopheles* larvae as the main parameter. Therefore, LST was involved as an important feature in fusing the results at the decision level, but other parameters played a less important role in the final results. On the other hand, some parameters were correlated with each other and provided common information. The magenta ellipses in Fig. 10 show the simultaneous occurrence of the peak of all the parameters. This is the most dangerous time for the growth of *Anopheles* mosquitoes, and then, if there are cases of the disease in the area, it will cause the

spread of malaria. Simultaneous temperature and precipitation provide suitable conditions for the growth of *Anopheles* larvae, but the important point was the presence of a high amount of LST (more than 45° C) from June to August in the study areas, which in the absence of cool shelter makes it impossible to grow and survive *Anopheles* mosquitoes.

Discussion

In this article, high-risk periods for three counties in Iran were monitored and predicted using remote sensing data in a seven-year time series through GEE. The three parameters of temperature, precipitation and vegetation as effective parameters in previous research were examined separately or in combination with remote sensing satellite observations and meteorological field observations during short periods. Given that the aim of this research was the prediction of high-risk times that would increase the abundance of *Anopheles*, it was necessary to monitor the climatic conditions of the study areas over a long period of time. Based on this, seven parameters of LST, NDVI, precipitation, soil moisture, ET and VH indices have been monitored over a seven-year period by processing time series of remote sensing data in GEE. Due to GEE's valuable capabilities in easy access and fast processing of remote sensing time series data, it was possible to monitor a variety of environmental parameters that directly or indirectly provide the suitable conditions for *Anopheles* mosquito growth and survival; and, consequently, malaria outbreaks in susceptible areas.

According to the results, obtained in Fig.10, two peaks in a year for each three study areas had been identified as high risk times. The first peak was from late winter to late spring, and the second peak was from late summer to mid-autumn. The co-occurrence of appropriate values of LST, precipitation, NDVI, soil moisture, ET and VCI would make this period of time

the most high-risk time in a year in the study areas. These results also demonstrate a correlation between ET, precipitation and soil moisture. This may be due to the subtropical climate of the study areas. Therefore, in this type of climate, one of these three parameters can be optimally extracted to investigate the prediction of abundance of *Anopheles* mosquitoes. During the summer months in June and July, precipitation, LST and high VCI were observed. But in this season, the temperature is above 40 degrees on average, which is not a suitable temperature for the growth and survival of *Anopheles*. Besides, if large pits and depressions are formed, e.g., through monsoon rains in the study areas, their stability will be low due to the high dryness of the regions. Pits and depressions will dry up due to surface evaporation and high permeability of dry soil, and, consequently, *Anopheles* larvae will not have enough time to grow in the aquatic environment. These conditions will be effective only for the growth of *Anopheles* larvae when the vegetation in the area is high and gardens and farmlands are available. Because these areas can be a cool shelter for the survival of *Anopheles,* and if water accumulates at the foot of trees and shrubs, they create a larval habitat. Therefore, over time, the larvae become adult mosquitoes (higher temperature in the appropriate temperature range accelerates this process) and cause the spread of malaria in the region.

In order to evaluate the accuracy of the estimated high-risk times in a year, field data of the abundance of *Anopheles* mosquitoes were needed. Due to the lack of access to appropriate entomological data in the regions, the previous three studies [29-31] conducted in the study areas had been used for final evaluation. The years studied in these three researches were neither rainy nor drought years and were consistent with the average climatic conditions over a seven-year period.

According to a study conducted by Edalat et al. [31] in Qaleh-Ganj County, the abundance of *Anopheles* mosquitoes began to increase in February and had been increasing until May, after that, the abundance rate is negative. Again, from September to November, the abundance of *Anopheles* mosquitoes increased and decreased rapidly in December. This statistic had been done for five different species of *Anopheles* mosquitoes, including *An. stephensi*, *An. culicifacies* s.l.*, An. superpictus* s.l.*, An. dthali* and *An. fluviatilis* s.l. All five species had similar behaviors in increasing and decreasing abundance.

The next study was conducted in Sarbaz County on four different species of *Anopheles* mosquitoes, including *An. stephensi*, *An. culicifacies* s.l., *An. superpictus s.l.*, *An. dthali* and *An. fluviatilis* s.l., from 2016 to 2017 [28]. Apart from *An. culicifacies*, three other species start to increase in abundance in early February up to April and then decrease until June. The abundance rate had increased again since September and had been decreasing since the beginning of November. In *An. culicifacies* species in both mentioned periods, it had increased one month earlier and decreased one month later. By comparing the results of the proposed method (Figure 9) with entomological data for Qaleh-Ganj and Bashagard counties, the accuracy of the predicted high-risk times was confirmed.

Nejati et al. [30] had done abundant counting only on one type of *Anopheles* species called *An. subpictus* in Sarbaz County. According to this research, three major peaks would be observed in 2015. The first peak began in February, peaking in March and declining in April. The second peak was seen in July and August, and finally, at the beginning of September, the third peak started and reached its maximum in early December.

By comparing the research results with the entomological data of Sarbaz County, two time periods from February to May and also from October to November were confirmed. But a

peak that occurred in August was not seen. It might be due to the fact that the amount of rain provides enough water reservoirs, in July, for *Anopheles* larvae, but the high temperature of that month pushes them to shelter anywhere in shadow; therefore, in August we see a marked increase in *Anopheles* population.

In previous researches, vegetation index such as NDVI has been used as a key factor in determining the location and abundance of *Anopheles* mosquitoes [3,46]. This case could be seen in the results of the two counties of Sarbaz and Bashagard, but in Qaleh-Ganj County, despite the low NDVI, the abundance of *Anopheles* mosquitoes had been increased from September to November. Accordingly, it would be important to consider other effective factors.

In addition, based on the proposed method, it is possible to estimate the maximum activity of *Anopheles* mosquitoes each year without the need for extensive entomological studies. Therefore, the exact time of spraying can be determined.

Conclusion

The results of this article demonstrated that in order to accurately predict high-risk times in a year for a specific area, sufficient knowledge of the climatic behavior of that area is very important. Also, using all the effective and optimal environmental parameters simultaneously will help to accurately predict the exact times of malaria outbreak for a region. With this method, it is possible to accurately and at low cost to predict the appropriate times for malaria vector control operations in different areas. GEE made it possible to analyze the time series of climatic data in the shortest time using its processing capability and easy access to a variety of free remote sensing data. Finally, these results will help to optimally select data with high spatial resolution that can better locate *Anopheles* habitats for growth and survival and give an overview

of the situation in dealing with the malaria outbreak in the region. It is recommended using the optimization method in future research in order to evaluate the results and selection of the effective parameters for each region and perform the final analysis without the need for user supervision.

Abbreviations

NDVI: Normalized Difference Vegetation Index;

LST: Land Surface Temperature;

GEE: Google Earth Engine;

PERSIANN-CDR: Precipitation Estimation from Remotely Sensed Information using Artificial Neural Networks - Climate Data Record;

NASA-USDA Enhanced SMAP: National Aeronautics and Space Administration-United States Department of Agriculture Enhanced Soil Moisture Active Passive;

ET: EvapoTranspiration;

MODIS: Moderate Resolution Imaging Spectroradiometer;

TCI: Thermal Condition Index;

VCI: Vegetation Condition Index;

Acknowledgment

The authors would like to thank the Iran National Science Foundation (INSF) for its financial support. Grant number: 98018439.

Authors' contributions

FY, MJVZ and AAHB designed the study. FY analyzed the data. FY wrote the manuscript. MJVZ and AAHB supervised the study and revised the manuscript. All authors reviewed and approved the final manuscript.

Funding

This study is supported by a grant to K.N. Toosi University of Technology from Iran National Science Foundation (INSF), Grant Number: 98018439.

Availability of data and materials

The data supporting the conclusions of this manuscript are included within the manuscript and are available from the corresponding author on reasonable request.

Declarations

Ethics approval and consent to participate

Not applicable.

Consent for publication

Not applicable.

Competing interests

The authors declare that they have no competing interests

Author details

[1] Ph.D. Student in Photogrammetry and Remote Sensing at K. N. Toosi University of Technology, Tehran, Iran; [2] Full Professor in Photogrammetry and Remote Sensing at K. N. Toosi University of Technology, Tehran, Iran; [3] Full Professor, Department of Medical Entomology & Vector Control, School of Public Health at Tehran Medical Science University, Tehran, Iran; [4] Full Professor in

Hydrology Civil engineering at K. N. Toosi University of Technology, Tehran, Iran; [5] Lecturer, School of Engineering at University of Newcastle Australia; [6] Assistant Professor in Photogrammetry and Remote sensing at Tafresh University, Arak, Iran.

References

[1] Herekar F, Iftikhar S, Nazish A, Rehman S. Malaria and the climate in Karachi: An eight year review. Pakistan J Med Sci. 2020;36(1):S33-S37. doi: 10.12669/pjms.36.ICON-Suppl.1712

[2] Thomson MC, Connor SJ. The development of malaria early warning systems for Africa. Trends Parasitol. 2001;17(9):438-45. doi: 10.1016/s1471-4922(01)02077-3.

[3] Abdelsattar A, Hassan AN. Assessment of malaria resurgence vulnerability in Fayoum, Egypt Using Remote Sensing and GIS. Egypt J Remote Sens Space Sci. 2021;24(1):77-84. doi: 10.1016/j.ejrs.2020.01.004

[4] Onyemaechi NE, Malann YD, Matur BM, Hassan SC. Impact of environmental factors on Anopheline larval density. South Asian J Parasitol. 2020;3:13-24.

[5] Marj AA, Mobasheri MR, VALADAN ZOEJ MJ, Rezaei Y, Abaei MR. Exploring the use of satellite images in the estimation of potential malaria outbreak regions. Environ Hazards. 2009;8(2):89-100.

[6] Wimberly MC, de Beurs KM, Loboda TV, Pan WK. Satellite observations and malaria: new opportunities for research and applications. Trends Parasitol. 2021; 37(6):525-537. doi: 10.1016/j.pt.2021.03.003

[7] Bationo CS, Gaudart J, Sokhna D, Cissoko M, Taconet P, Ouedraogo B, Somé A, Zongo I, Dieudonné SD, Tougri G, Dabiré RK. Spatio-temporal analysis and prediction of malaria cases using remote sensing meteorological data in Diébougou health district, Burkina Faso, 2016-2017. Sci Rep. 2021. 11, 20027. doi: 10.1038/s41598-021-99457-9.

[8] Ferrão JL, Mendes JM, Painho M. Modelling the influence of climate on malaria occurrence in Chimoio Municipality, Mozambique. Parasit Vectors. 2017;10(1):1-2. doi: 10.1186/s13071-017-2205-6

[9] World Health Organization. World malaria report 2020: 20 years of global progress and challenges. InWorld malaria report 2020: 20 years of global progress and challenges 2020.

[10] Minale AS, Alemu K. Mapping malaria risk using geographic information systems and remote sensing: The case of Bahir Dar City, Ethiopia. Geospat Health. 2018;13(1). doi: 10.4081/gh.2018.660

[11] Adeola AM, Botai JO, Olwoch JM, Rautenbach HC, Adisa OM, De Jager C, Botai CM, Aaron M. Predicting malaria cases using remotely sensed environmental variables in Nkomazi, South Africa. Geospat Health. 2019;14(1). doi: 10.4081/gh.2019.676

[12] Midekisa A, Senay G, Henebry GM, Semuniguse P, Wimberly MC. Remote sensing-based time series models for malaria early warning in the highlands of Ethiopia. Malaria J. 2012;11(1):1-0. doi: 10.1186/1475-2875-11-165

[13] Stresman GH. Beyond temperature and precipitation: ecological risk factors that modify malaria transmission. Acta Trop. 2010;116(3):167-72. doi: 10.1016/j.actatropica.2010.08.005

[14] Aytekin S, Aytekin AM, Alten B. Effect of different larval rearing temperatures on the productivity (Ro) and morphology of the malaria vector *Anopheles superpictus* Grassi (Diptera: Culicidae) using geometric morphometrics. J Vector Ecol. 2009;34(1):32-42. doi: 10.1111/j.1948-7134.2009.00005.x

[15] Bayoh MN, Lindsay SW. Temperature-related duration of aquatic stages of the Afrotropical malaria vector mosquito *Anopheles gambiae* in the laboratory. Med Vet Entomol. 2004;18(2):174-9. doi: 10.1111/j.0269-283X.2004.00495.x

[16] Lyons CL, Coetzee M, Chown SL. Stable and fluctuating temperature effects on the development rate and survival of two malaria vectors, *Anopheles arabiensis* and *Anopheles funestus*. Parasit Vector. 2013;6(1):1-9. doi: 10.1186/1756-3305-6-104

[17] Baig S, Sarfraz MS. Spatio-temporal analysis to predict environmental influence on Malaria. Int Arch Photogramm Remote Sens Spat Inf Sci-ISPRS Arch. 2018;42(3):2615-7. doi: 10.5194/isprs-archives-XLII-3-2615-2018

[18] Sewe MO, Tozan Y, Ahlm C, Rocklöv J. Author Correction: Using remote sensing environmental data to forecast malaria incidence at a rural district hospital in Western Kenya. Sci Rep. 2018;8(1):1-. doi: 10.1038/s41598-018-23241-5

[19] Mousam A, Maggioni V, Delamater PL, Quispe AM. Using remote sensing and modeling techniques to investigate the annual parasite incidence of malaria in Loreto, Peru. Adv Water Resour. 2017;108:423-38. doi: 10.1016/j.advwatres.2016.11.009

[20] Mazher MH, Iqbal J, Mahboob MA, Atif I. Modeling spatio-temporal malaria risk using remote sensing and environmental factors. Iranian J Publ Health. 2018;47(9):1281-1291.

[21] Rahman A, Kogan F, Roytman L. Analysis of malaria cases in Bangladesh with remote sensing data. The American journal of tropical medicine and hygiene. 2006;74(1):17-19.

[22] Nizamuddin M, Kogan F, Dhiman R, Guo W, Roytman L. Modeling and forecasting malaria in Tripura, INDIA using NOAA/AVHRR-based vegetation health indices. Int J Remot Sens Appl. 2013;3(3):108-16.

[23] Kogan F. 1981–2019 Vegetation Health Trends Assessing Malaria Conditions During Intensive Global Warming. In book: Remote Sensing for Malaria. 2020; 219-263.

[24] Manyangadze T, Chimbari MJ, Macherera M, Mukaratirwa S. Micro-spatial distribution of malaria cases and control strategies at ward level in Gwanda district, Matabeleland South, Zimbabwe. Malaria J. 2017;16(1):1-1. doi: 10.1186/s12936-017-2116-1

[25] Parselia E, Kontoes C, Tsouni A, Hadjichristodoulou C, Kioutsioukis I, Magiorkinis G, Stilianakis NI. Satellite earth observation data in epidemiological modeling of malaria, dengue and West Nile virus: a scoping review. Remote Sens. 2019;11(16):1862. doi: 10.3390/rs11161862

[26] Schmieder M, Holl F, Fotteler ML, Örtl M, Buchner E, Swoboda W. Remote sensing and on-site characterization of wetlands as potential habitats for malaria vectors–A pilot study in southern Germany. In: 2020 IEEE Global Humanitarian Technology Conference (GHTC). 2020;1-4. doi: 10.1109/GHTC46280.2020.9342952.

[27] Karthikeyan R, Rupner RN, Koti SR, Jaganathasamy N, Malik YS, Sinha DK, Singh BR, Vinodh Kumar OR. Spatio-temporal and time series analysis of bluetongue outbreaks with environmental factors extracted from Google Earth Engine (GEE) in Andhra Pradesh, India. Transbound Emerg Dis. 2021, 68(6): 3631-3642. doi: 10.1111/tbed.13972

[28] Tamiminia H, Salehi B, Mahdianpari M, Quackenbush L, Adeli S, Brisco B. Google Earth Engine for geo-big data applications: A meta-analysis and systematic review. ISPRS J Photogramm Remote Sens. 2020;164:152-70. doi: 10.1016/j.isprsjprs.2020.04.001

[29] Sanei-Dehkordi A, Soleimani-Ahmadi M, Jaberhashemi SA, Zare M. Species composition, seasonal abundance and distribution of potential anopheline vectors in a malaria endemic area of Iran: field assessment for malaria elimination. Malaria J. 2019 Dec;18(1):1-9. doi: 10.1186/s12936-019-2795-x

[30] Nejati J, Saghafipour A, Vatandoost H, Moosa-Kazemi SH, Motevalli Haghi A, Sanei-Dehkordi A. Bionomics of *Anopheles subpictus* (Diptera: Culicidae) in a malaria endemic area, southeastern Iran. J Med Entomol. 2018;55(5):1182-7. doi: 10.1093/jme/tjy079

[31] Edalat H, Mahmoudi M, Sedaghat MM, Moosa-Kazemi SH, Kheirandish S. Ecology of malaria vectors in an endemic area, Southeast of Iran. J Arthropod-Borne Dis. 2020;14(4):325-343. doi: 10.18502%2Fjad.v14i4.5270

[32] Vatandoost H, Mashayekhi M, Abaie MR, Aflatoonian MR, Hanafi-Bojd AA, Sharifi I. Monitoring of insecticides resistance in main malaria vectors in a malarious area of Kahnooj district, Kerman province, southeastern Iran. J Vector-borne Dis. 2005;42(3):100-8.

[33] Hanafi-Bojd AA, Vatandoost H, Oshaghi MA, Charrahy Z, Haghdoost AA, Zamani G, Abedi F, Sedaghat MM, Soltani M, Shahi M, Raeisi A. Spatial analysis and mapping of malaria risk in an endemic area, south of Iran: a GIS based decision making for planning of control. Acta Trop. 2012;122(1):132-7. doi: 10.1016/j.actatropica.2012.01.003

[34] Hanafi-Bojd AA, Vatandoost H, Oshaghi MA, Haghdoost AA, Shahi M, Sedaghat MM, Abedi F, Yeryan M, Pakari A. Entomological and epidemiological attributes for malaria transmission and implementation of vector control in southern Iran. Acta Trop. 2012;121(2):85-92. doi: 10.1016/j.actatropica.2011.04.017

[35] Vatandoost H, Raeisi A, Saghafipour A, Nikpour F, Nejati J. Malaria situation in Iran: 2002–2017. Malaria journal. 2019;18(1):1-7. doi: 10.1186/s12936-019-2836-5

[36] Abbasi, M., Hanafi-Bojd, A.A., Oshaghi, M.A., Vatandoost, H., Yaghoobi-Ershadi, M.R. and Hazratian, T. Laboratory estimation of growth degree-day (GDD) developmental requirements of *Anopheles stephensi* (Diptera: Culicidae). Proceedings of the 2nd International Congress of Climate Change and Vector-Borne Diseases, Shiraz, Iran. 2018; https://civilica.com/doc/965827.

[37] Duggin MJ, Piwinski D. Recorded radiance indices for vegetation monitoring using NOAA AVHRR data; atmospheric and other effects in multitemporal data sets. Appl Opt. 1984;23(15):2620-3. doi: 10.1364/AO.23.002620

[38] Courault D, Seguin B, Olioso A. Review to estimate evapotranspiration from remote sensing data: some examples from the simplified relationship to the use of mesoscale atmospheric models. In: ICID workshop on remote sensing of ET for large regions. 2003; 17:1-18.

[39] Lai S, Leone F, Zoppi C. Spatial distribution of surface temperature and land cover: A study concerning Sardinia, Italy. Sustainability. 2020;12(8):3186. doi: 10.3390/su12083186.

[40] Ashouri H, Hsu KL, Sorooshian S, Braithwaite DK, Knapp KR, Cecil LD, Nelson BR, Prat OP. PERSIANN-CDR: Daily precipitation climate data record from multisatellite observations for hydrological and climate studies. Bull Am Meteorol Soc. 2015;96(1):69-83. doi: 10.1175/BAMS-D-13-00068.1

[41] Sazib N, Mladenova I, Bolten J. Leveraging the Google Earth Engine for drought assessment using global soil moisture data. Remote Sens. 2018;10(8):1265. doi: 10.3390/rs10081265.

[42] Han Y, Li Z, Huang C, Zhou Y, Zong S, Hao T, Niu H, Yao H. Monitoring droughts in the Greater Changbai Mountains using multiple remote sensing-based drought indices. Remote Sens. 2020;12(3):530. doi: 10.3390/rs12030530

[43] Wei W, Zhang J, Zhou L, Xie B, Zhou J, Li C. Comparative evaluation of drought indices for monitoring drought based on remote sensing data. Environ Sci Pollut Res. 2021;28(16):20408-25. doi: 10.1007/s11356-020-12120-0

[44] Kogan FN. Global drought watch from space. Bull Am Meteorol Soc. 1997;78(4):621-36. doi: 10.1175/1520-0477(1997)078%3C0621:GDWFS%3E2.0.CO;2

[45] Running SW, Mu Q, Zhao M, Moreno A. MODIS global terrestrial evapotranspiration (ET) product (NASA MOD16A2/A3) NASA earth observing system MODIS land algorithm. NASA: Washington, DC, USA. 2017.

[46] Palaniyandi M. The red and infrared IRS WiFS satellite data for mapping of Malaria and JE Vector mosquito breeding habitats. J Geophys Remote Sens. 2014;3(126):2169-0049. doi: 10.4172/2169-0049.1000126

Figures

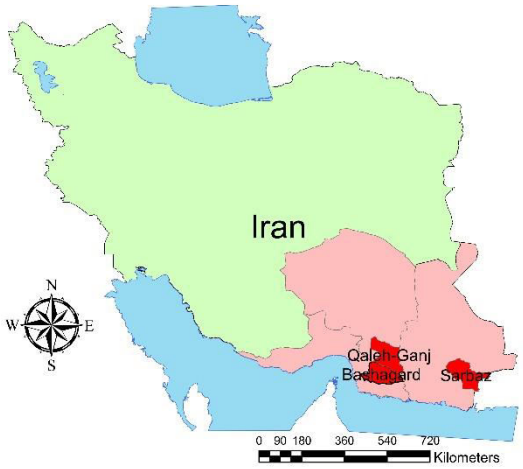

Fig. 1 Three study areas including the counties of Qaleh-Ganj, Sarbaz and Bashagard (red) located in the three provinces of Kerman, Sistan and Baluchestan and Hormozgan, respectively (pink) in Iran (green)

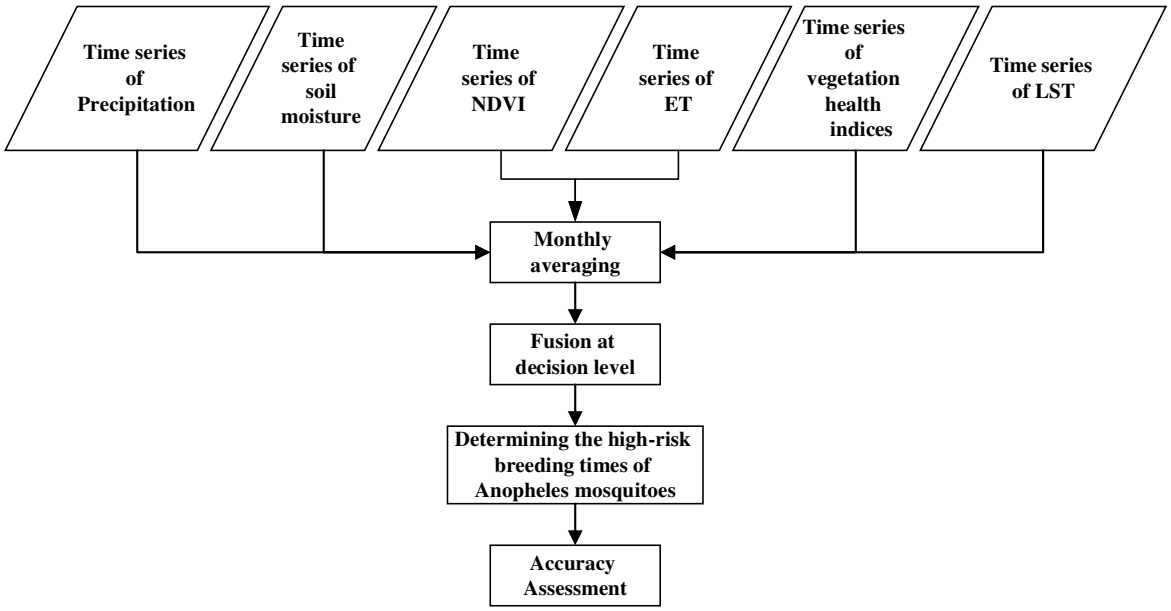

Fig. 2 Flowchart of the steps of the proposed method

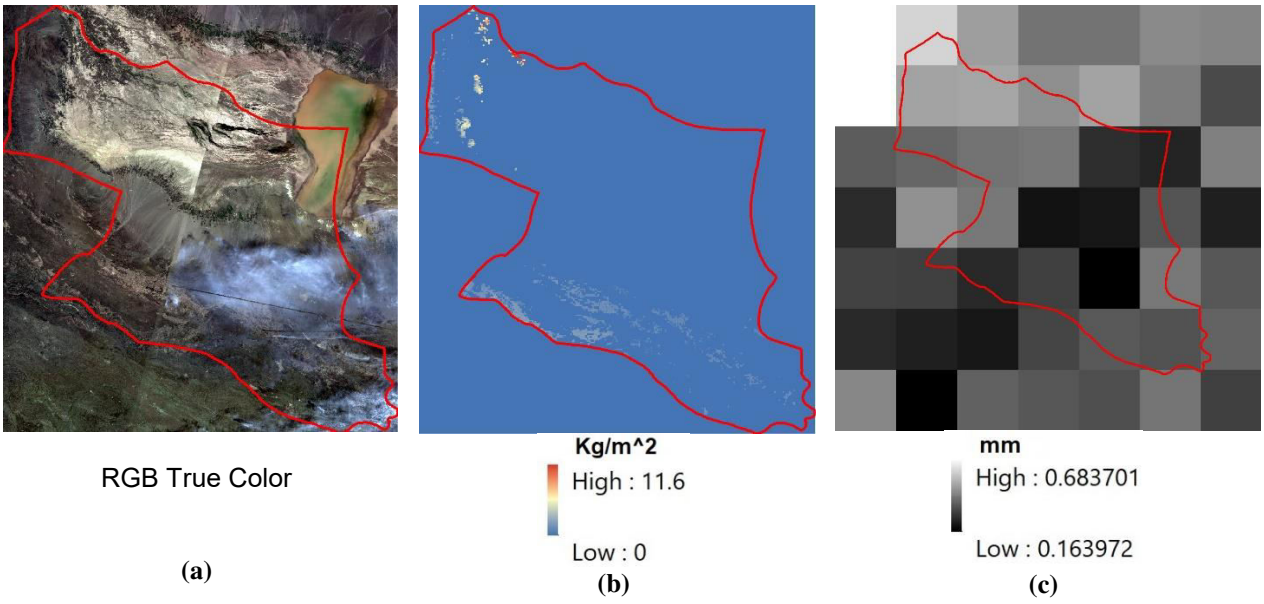

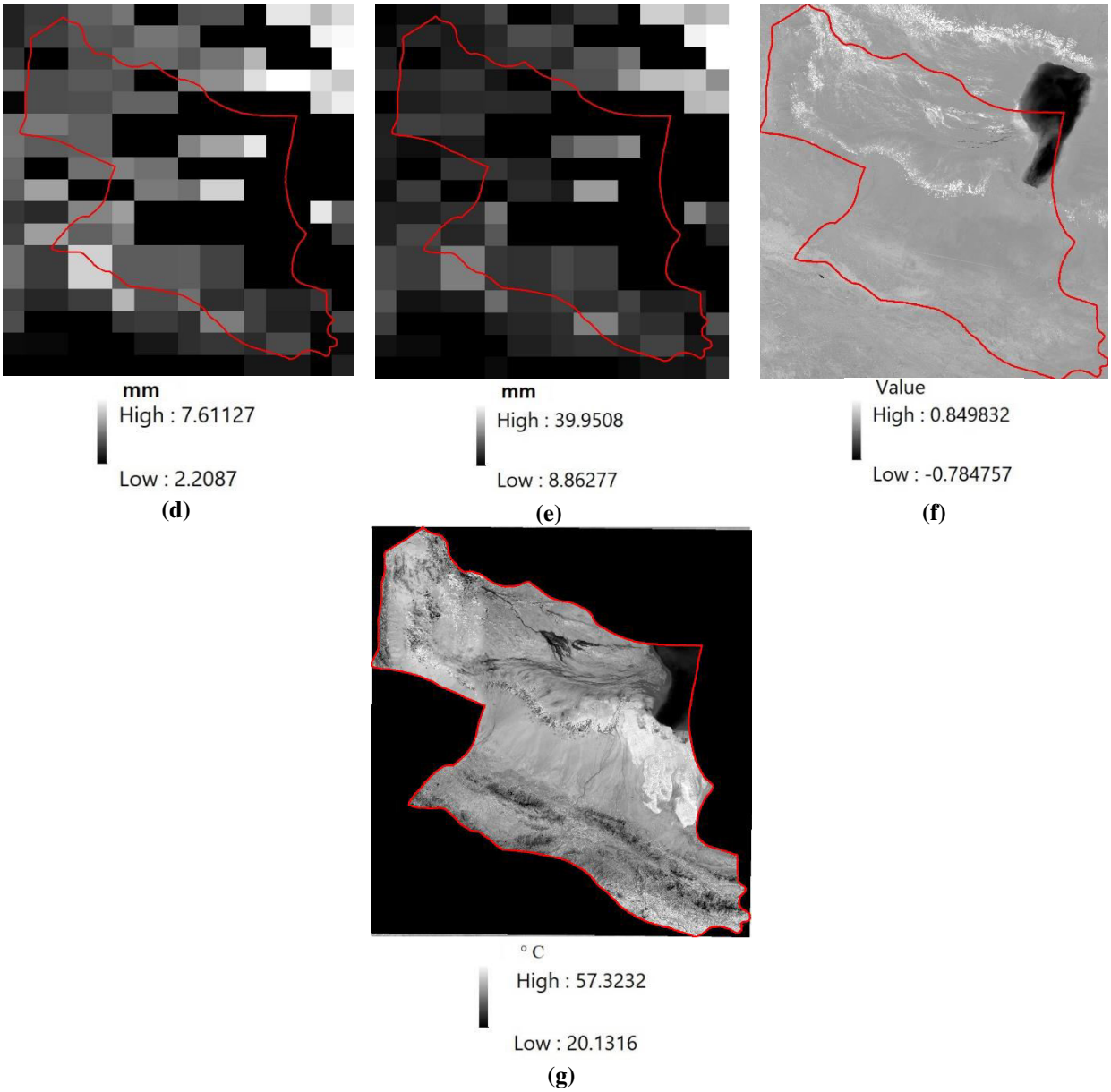

Fig. 3 Sample data from Qaleh-Ganj county (Red Boundary) acquired in April 2020 (**a**) RGB true color (**b**) ET (**c**) Precipitation (**d**) SSM (**e**) SUSM (**f**) NDVI (**g**) LST

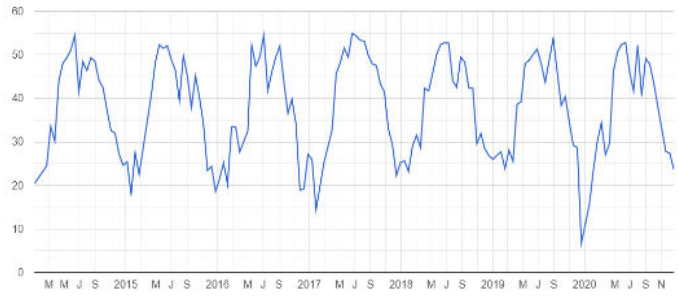

(a)

(b)

(c)

Fig. 4 LST time series of (**a**) Qaleh-Ganj, (**b**) Sarbaz and (**c**) Bashagard, Iran, 2014-2021

M: May, J: July, S : September

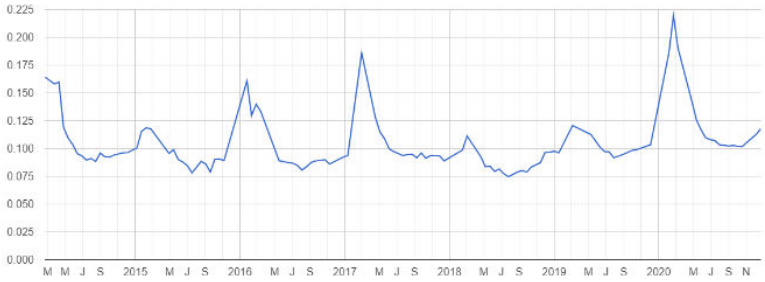

(a)

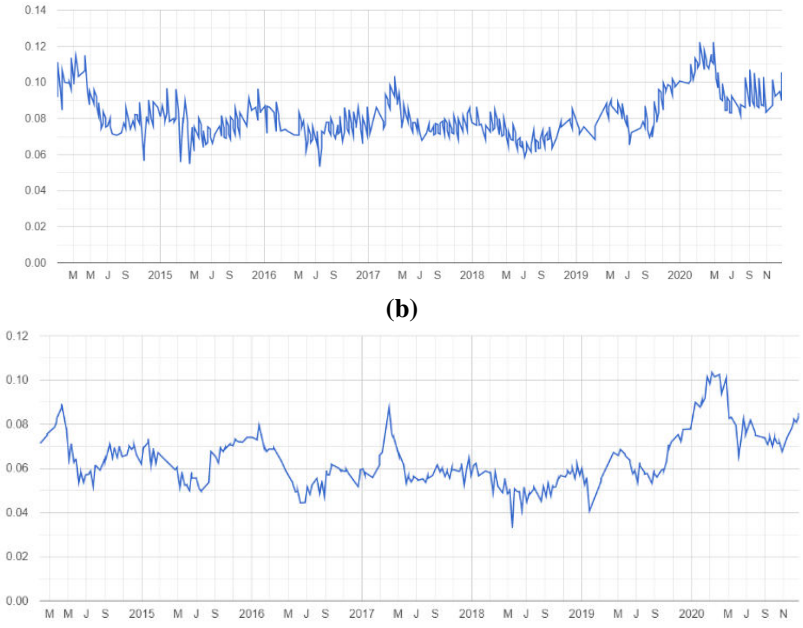

(b)

(c)

Fig. 5 NDVI time series of (**a**) Qaleh-Ganj, (**b**) Sarbaz and (**c**) Bashagard, Iran, 2014-2021

M: May, J: July, S: September

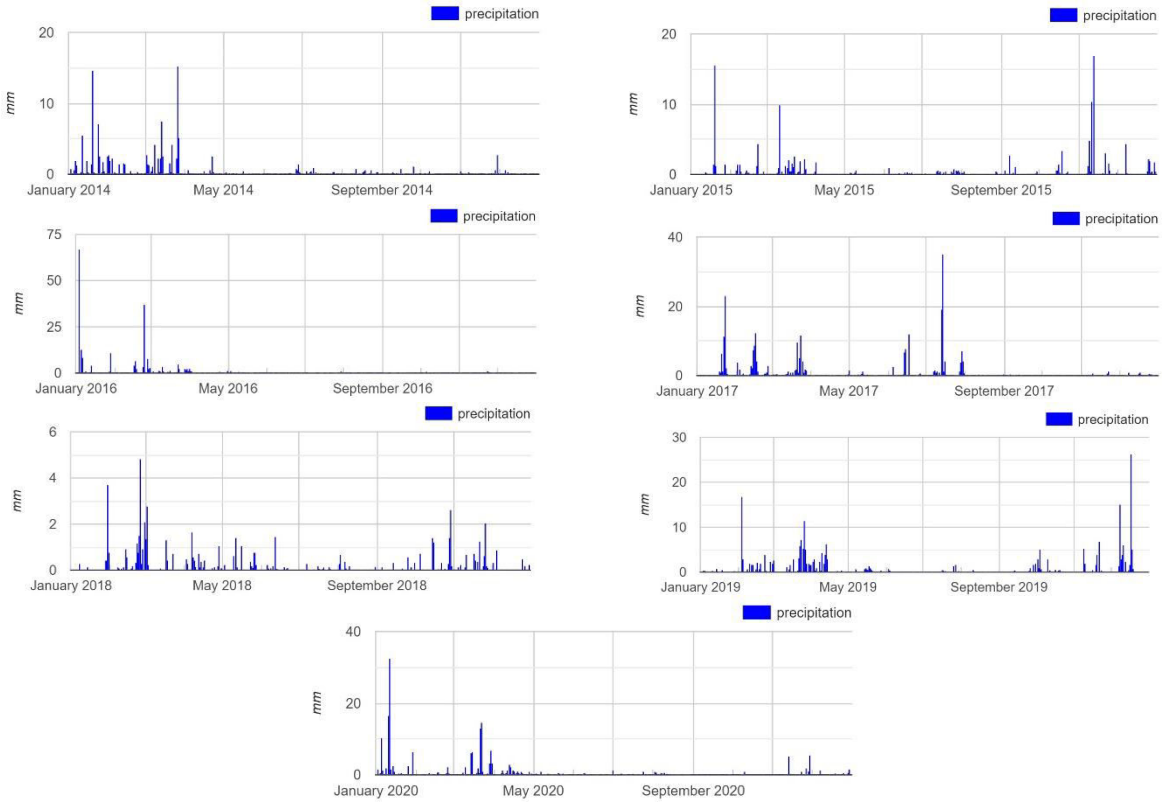

(a)

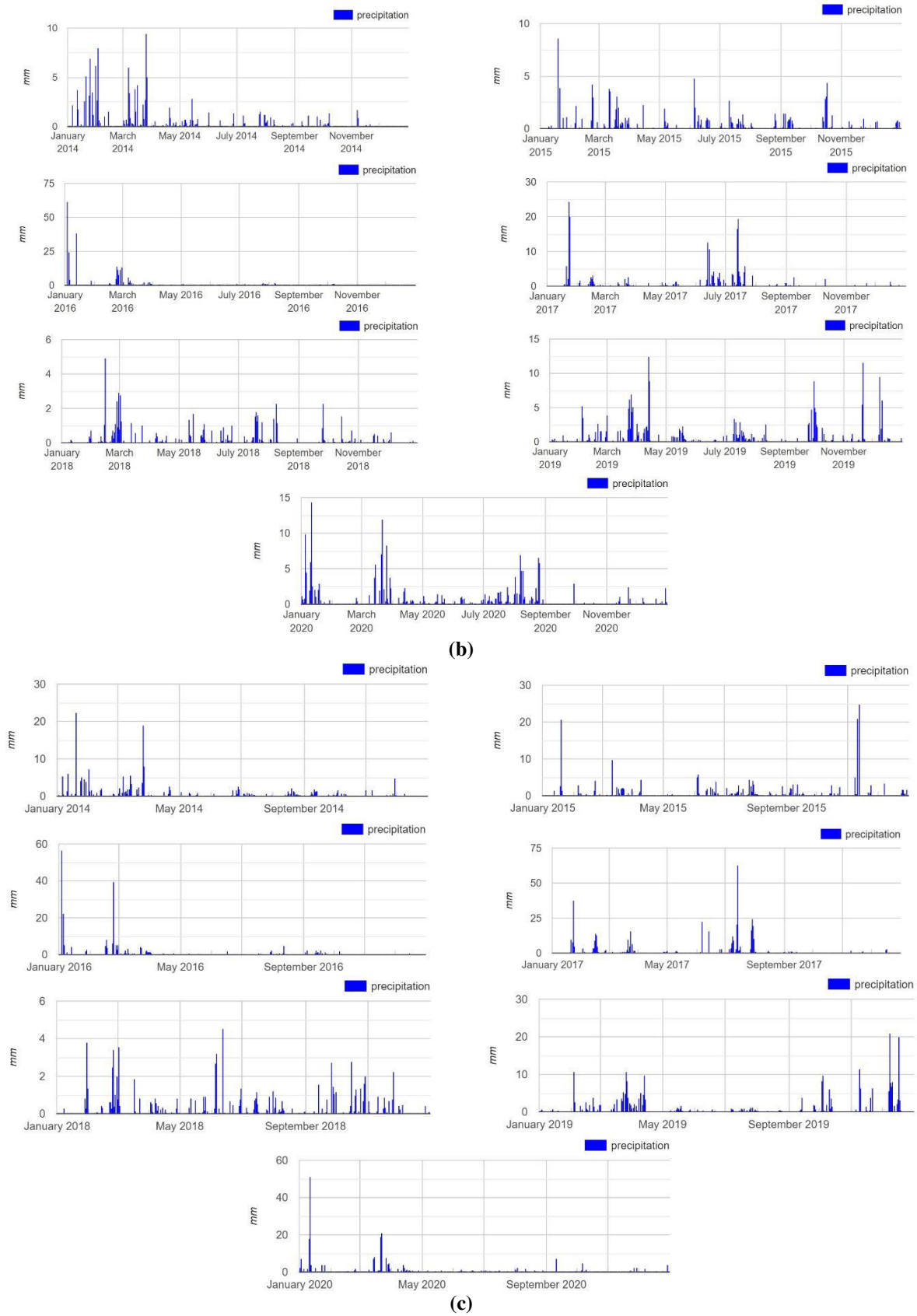

Fig. 6 Precipitation time series in Qaleh-Ganj (**a**), Sarbaz (**b**) and Bashagard (**c**), Iran, 2014-2021

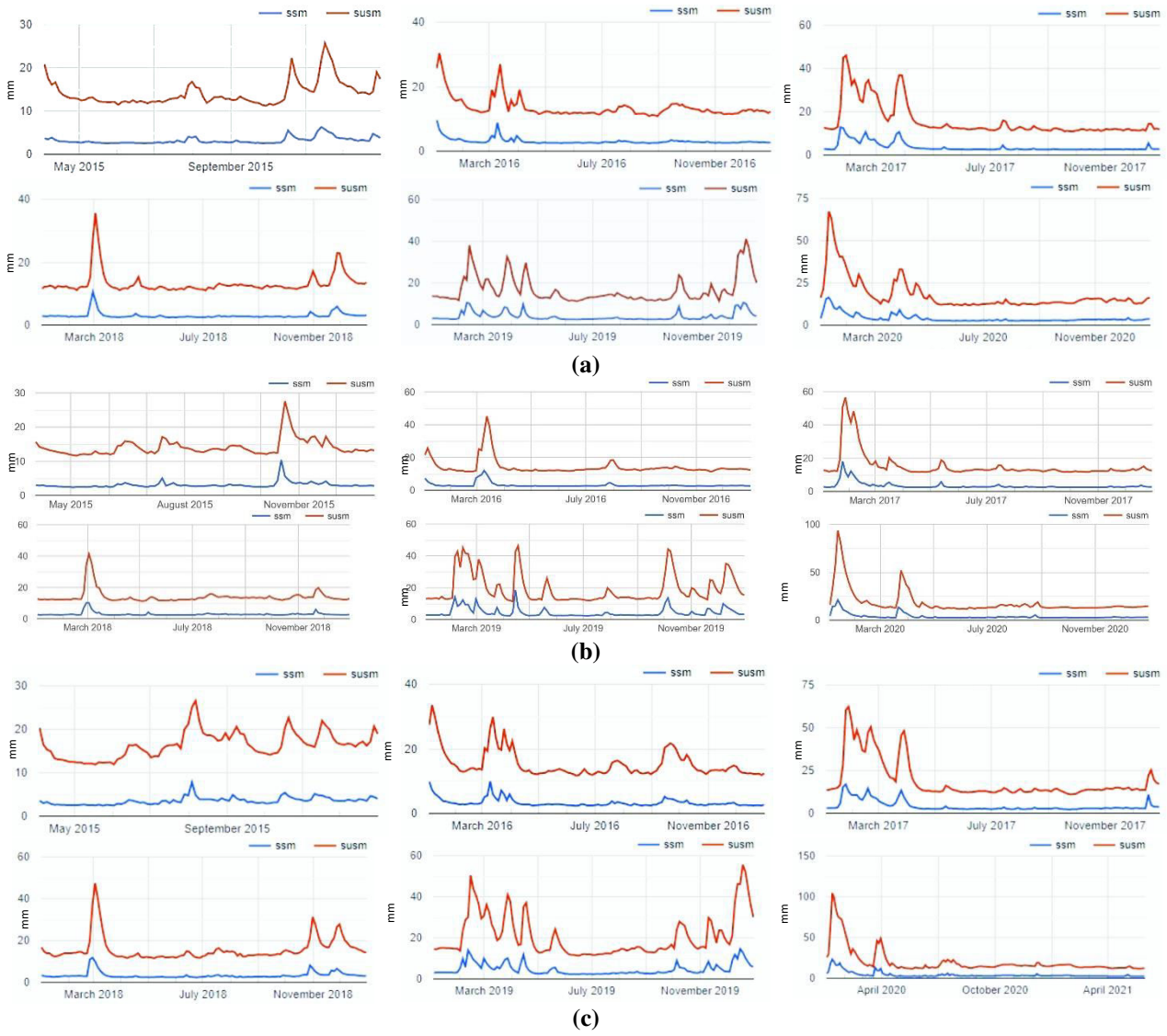

Fig. 7 Soil moisture time series of Qaleh-Ganj (**a**), Sarbaz (**b**) and Bashagard (**c**), Iran, 2015-2021

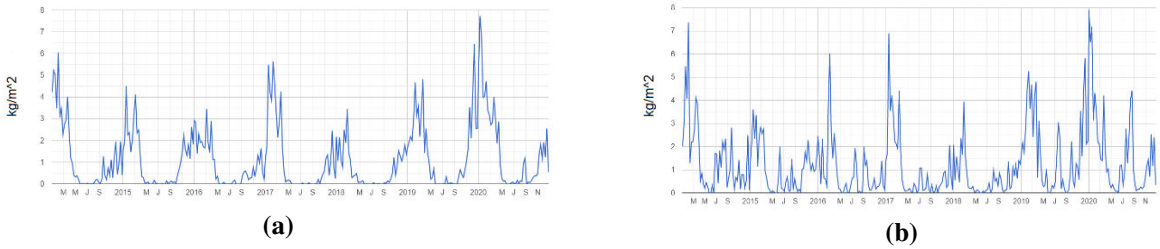

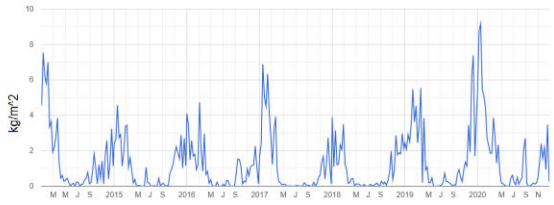

(c)

Fig. 8 ET time series of Qaleh-Ganj (**a**), Sarbaz (**b**) and Bashagard (**c**), Iran, 2014-2021

M: May, J: July, S: September

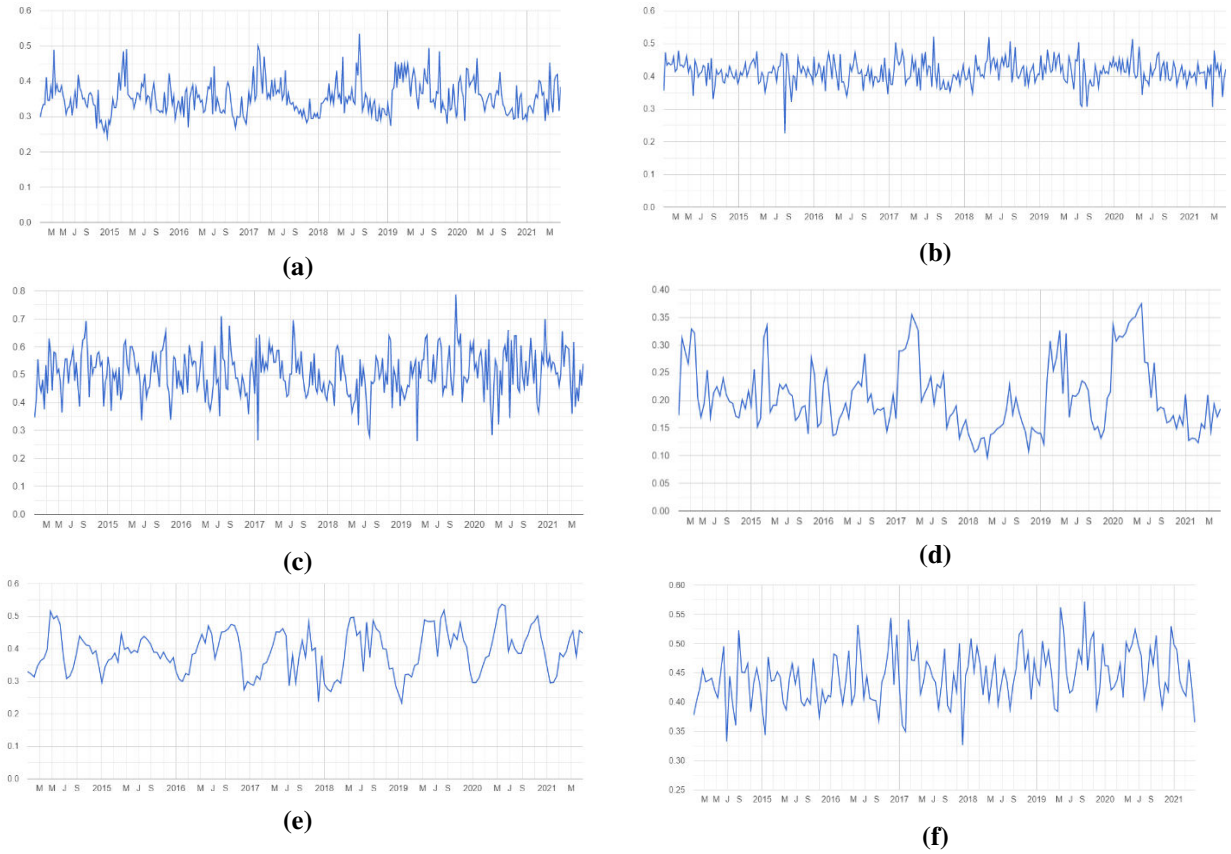

(a) **(b)** **(c)** **(d)** **(e)** **(f)**

Fig. 9 TCI time series of Qaleh-Ganj (**a**), Sarbaz (**b**) and Bashagard (**c**); VCI time series of Qaleh-Ganj (**d**), Sarbaz (**e**) and Bashagard (**f**), Iran, 2014-2021

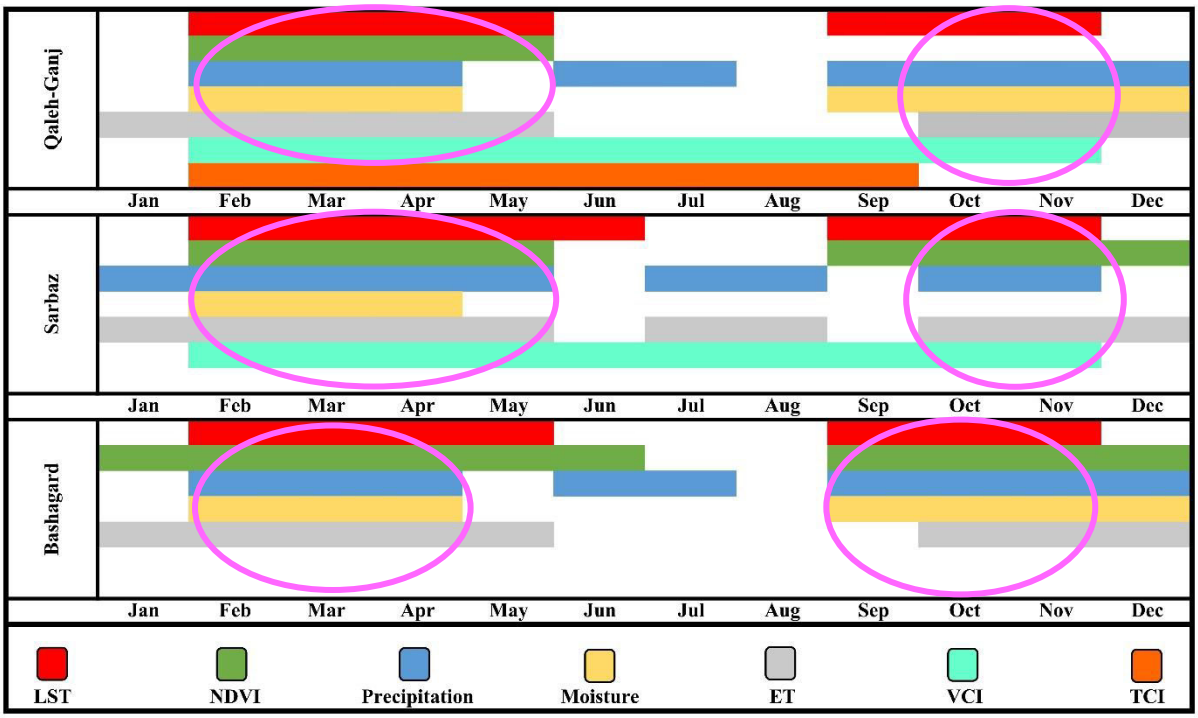

Fig. 10 Temporal prediction based on the averaging of effective parameteres in increasing the Anopheles abundance over a period of seven years. Pink ellipses indicate dangerous times in a year for study areas.

Tables

Table 1 Specifications of the data used

Data	Spatial Resoultion	Temporal Resolution
Landsat8 OLI/TIRS	• Visible and near infrared bands: 30 m • Thermal bands: 100 m	16-day
PERSIANN-CDR	27830 m	Daily
MOD16A2 Terra MODIS	500 m	8-day

NASA-USD Enhanced SMAP	10000 m	3-day

Table 2 Emissivity values based on NDV

NDVI	LSE
NDVI< -0.185	0.955
-0.185≤NDVI<0.157	0.985
0.157≤NDVI≤0.727	$1.009 + 0.047 \times \ln(NDVI)$
NDVI≥0.727	0.990

Supplementary Files

This is a list of supplementary files associated with this preprint. Click to download.

- graphicalabstract.pdf